SUPPLEMENTARY FIGURES

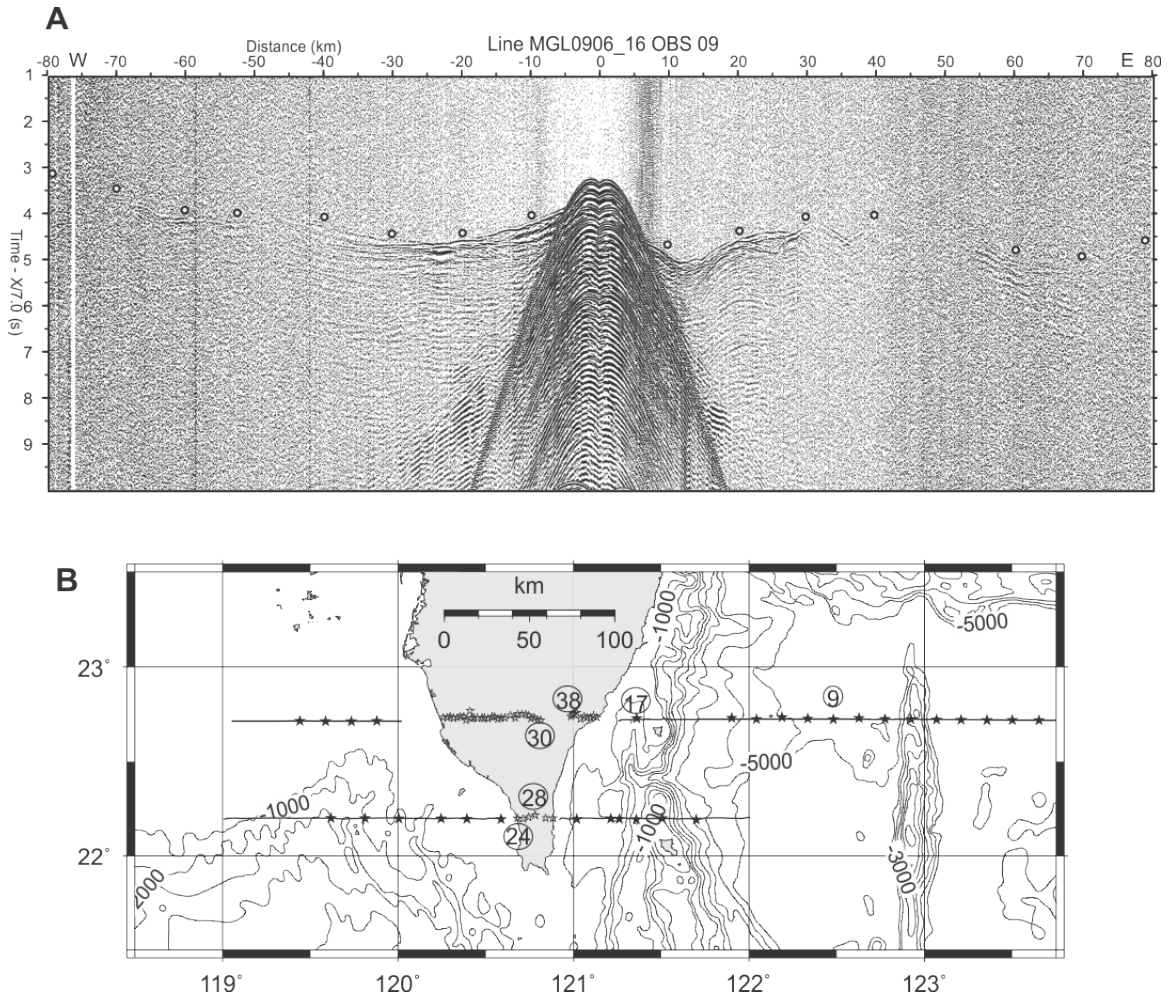

Figure DR1. MGL0906_16 OBS 09 data example and instrument location map. A) This OBS record section, displayed using a reduction velocity of 7.0 km/s, shows that first arrivals are interpretable up to 80 km east and west of this instrument. Small, open circles are placed just above first arrivals. The absence of arrivals near 50 km is due to rough morphology and complex structure across Gagua ridge. B) Map showing location of data example instrument in part A and for examples in subsequent supplementary figures. Instrument locations are stars with circled numbers identifying the specific instruments.

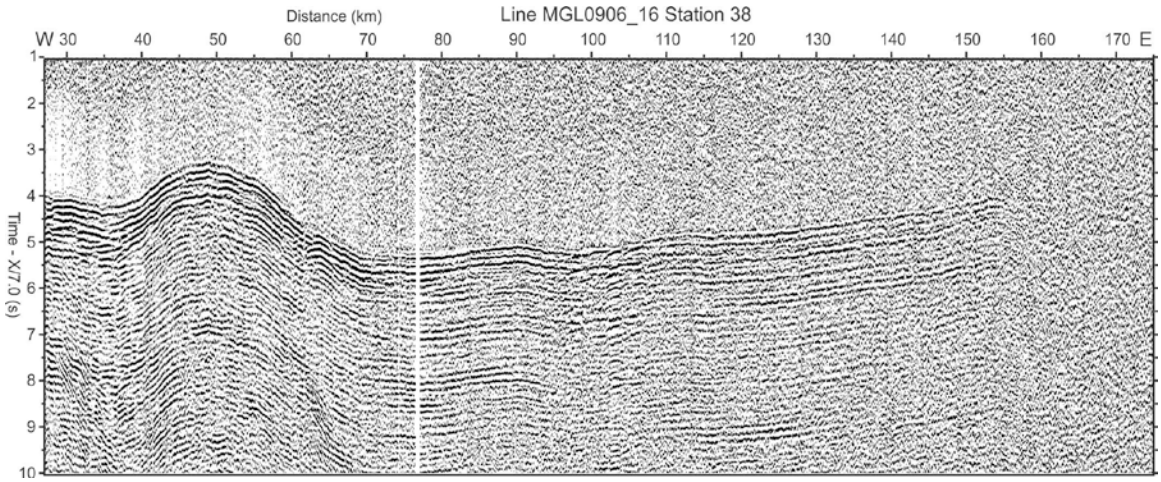

Figure DR2. MGL0906_16 Land station 38 data example. This land station record section of marine sources, displayed using a reduction velocity of 7.0 km/s, shows that first arrivals are interpretable up to 155 km east of this instrument. The early arrival times centred at 50 km mark the crest of the North Luzon arc. Location of line and land station is shown in fig. DR1B.

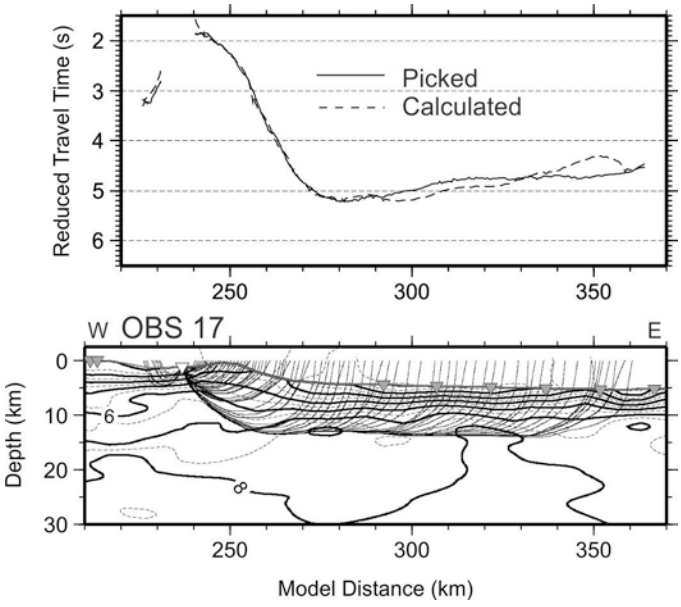

Figure DR3. MGL0906_16 Ray tracing and data fit diagrams. This diagram shows ray coverage and data fit for OBS 17, the first OBS offshore Taiwan (see fig. 1). Arrivals were picked to offsets of 120 km, but rays traced to this instrument are limited to depths

< 15 km due to the oceanic lithosphere. The data fit diagram is displayed with time reduced at 7 km/s. Location of line and OBS is shown in fig. DR1B.

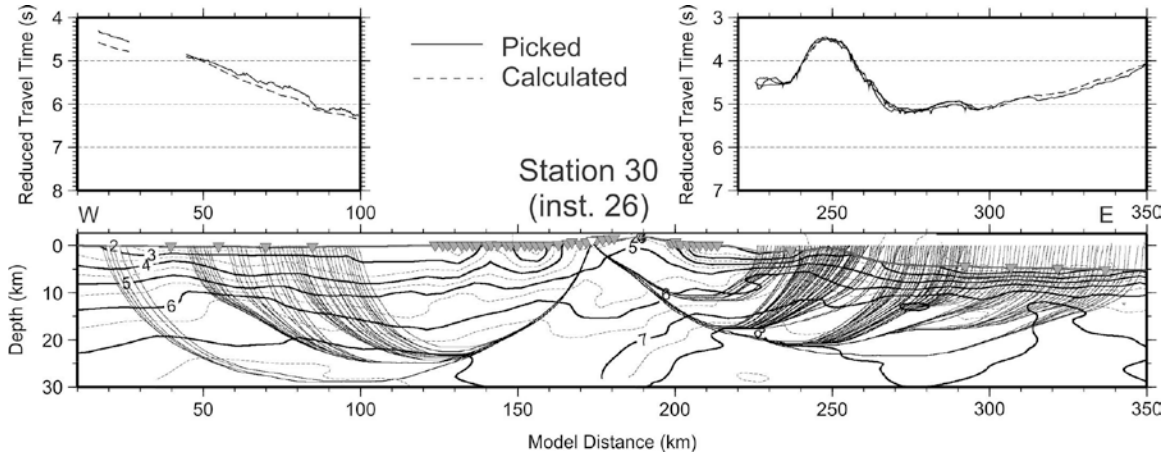

Figure DR4. Land station 30 ray tracing and data fit diagrams. Ray coverage and data fit to land station 30 from marine source positions both west and east of Taiwan. Dense coverage to the east is from two passes of shooting during separate OBS recording (120 m source spacing) and reflection acquisition (50 m spacing). Location of line and land station is shown in fig. DR1B.

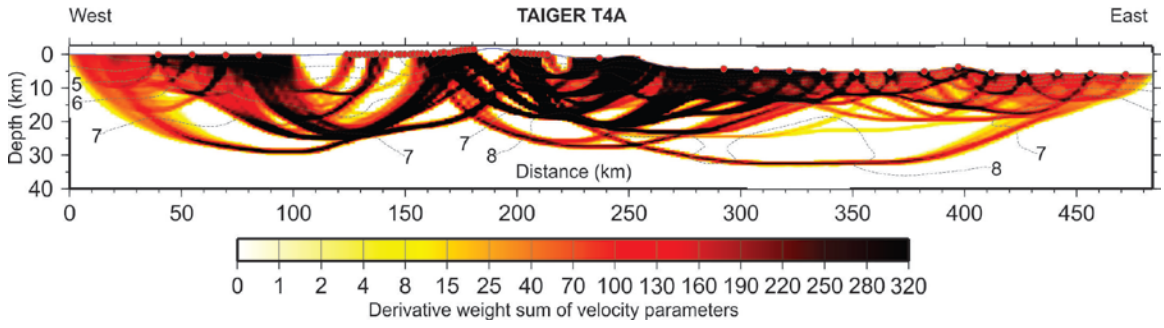

Figure DR5. Derivative weight sum (DWS) for the last iteration of the travel time inversion for T4A. The ray densities increase dramatically toward the center of the model due to the high-quality of the land stations, which recorded arrivals from both east

and west of the island. Densities were further increased on the east side because most of this profile was shot two times, but at different shot intervals optimized for reflection and OBS data sets. Many land stations recorded arrivals from the distant eastern portion of the profile at offsets of 250 to 300 km, which sampled deep into the oceanic mantle east of Taiwan. The zone of underplating at 20-30 km depth beneath western Taiwan is also well sampled. Velocity model contours are dashed for reference; OBS and land stations are marked by small red circles.

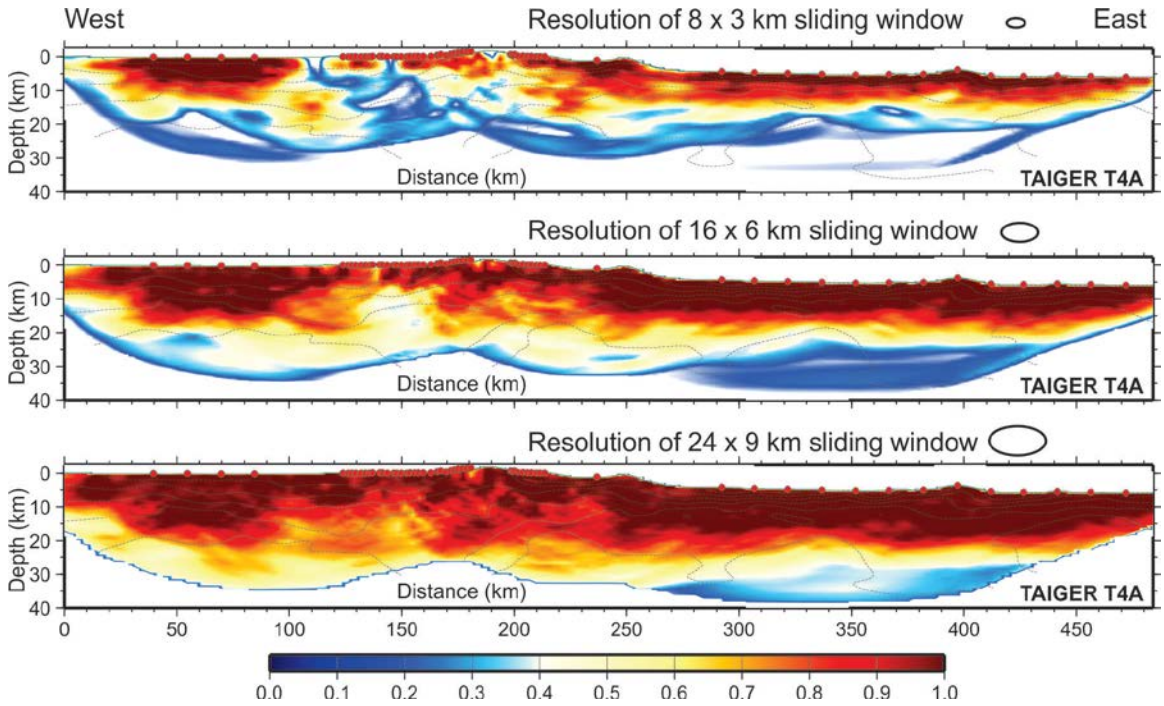

Figure DR6. Resolving power of the inversion estimated from the full resolution matrix for T4A. The resolution matrix is multiplied by sliding, elliptical windows of three different sizes to estimate how well objects of these sizes are resolved in the tomographic inversion. From top to bottom we use horizontally elongated ellipses of 8x3 km, 16x6 km, and 24x9 km. Areas with resolution values of 0.5 or greater are considered to be

sufficiently imaged. The plots for smaller sliding windows reveal some of the poorly resolved areas where there were larger spaces between instruments or poorer quality recordings, for example, X=110 km, X=145 km, and X=190 km. However, longer offset rays are able to define larger objects below these areas and throughout the model to about 30 km depth.

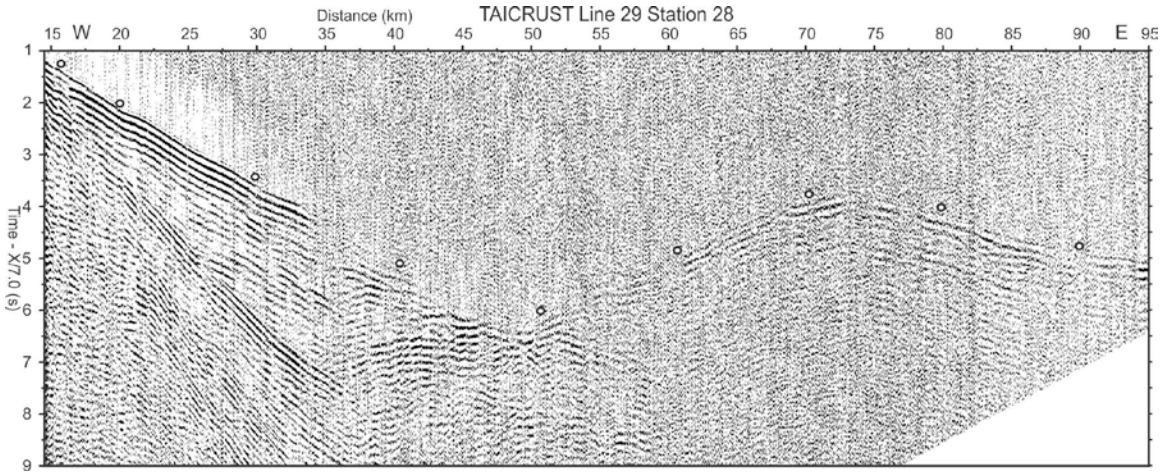

Figure DR7. T2933 Line 29, station 28 land data example. This record section, displayed using time reduced by a 7.0 km/s velocity, shows first arrivals from just east of Hengchun Peninsula to source positions east of North Luzon arc (centered at 73 km). Small open circles are placed just above first arrivals. These arrivals to offsets of 95 km sample the crustal and upper mantle structure below and east of the peninsula. Location of line and land station is shown in fig. DR1B. Note that examples of OBS data along this profile are published in ref. 22.

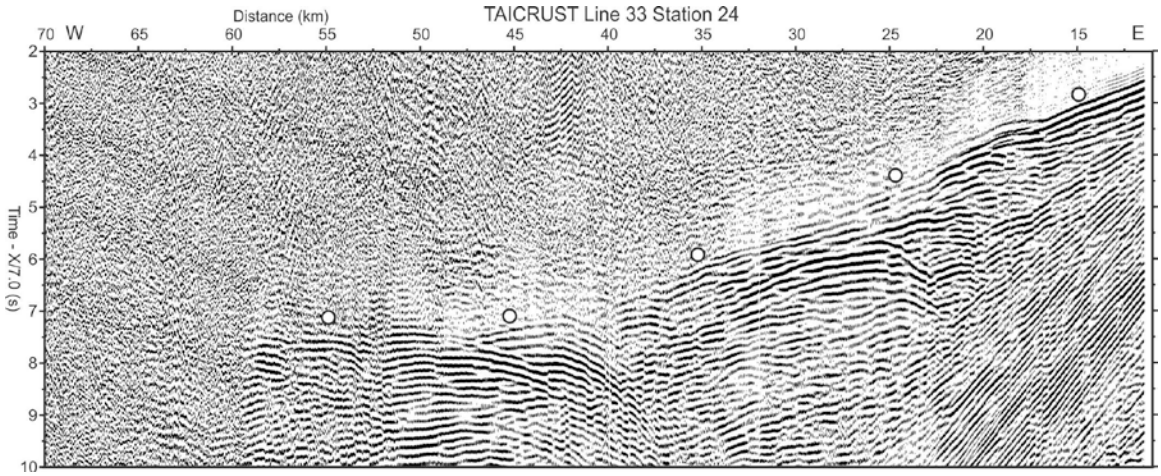

Figure DR8. T2933 Line 33, station 24 land data example. This record section, displayed using time reduced by a 7.0 km/s velocity, shows first arrivals from source positions west of the Hengchun Peninsula. Small open circles are placed just above first arrivals. These arrivals sample the crust and upper mantle below and west of the peninsula. Location of line and land station is shown in fig. DR1B.

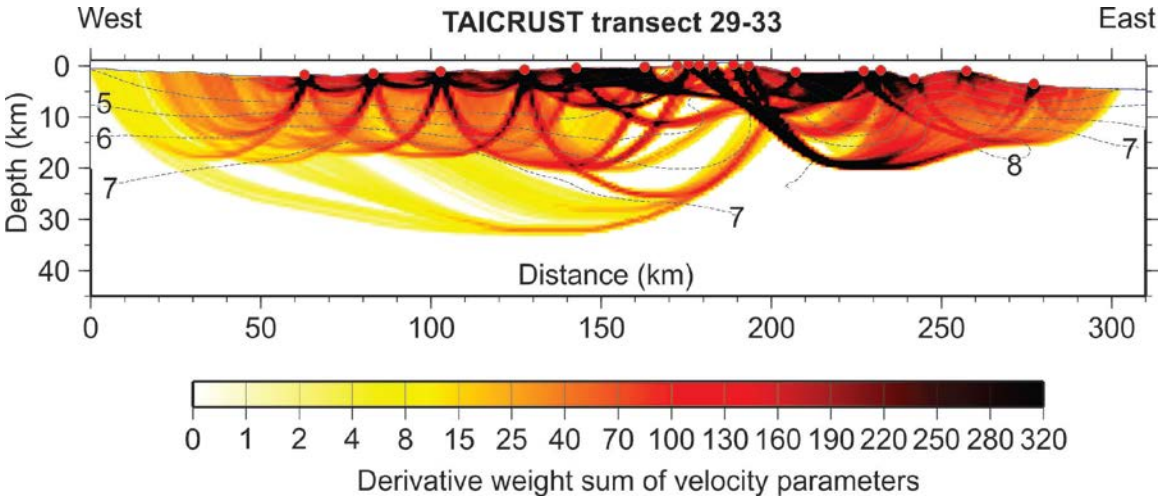

Figure DR9. Derivative weight sum (DWS) for the last iteration of the travel time inversion for T2933. The highest ray densities occur in the sedimentary section and upper crust, except for the upper mantle structure in the range X= 200-250 km. Land

stations provide critical sampling of the high-velocity prism core, as do rays that undershoot the Hengchun Peninsula. Velocity model contours are dashed for reference; OBS and land stations are marked by small red circles.

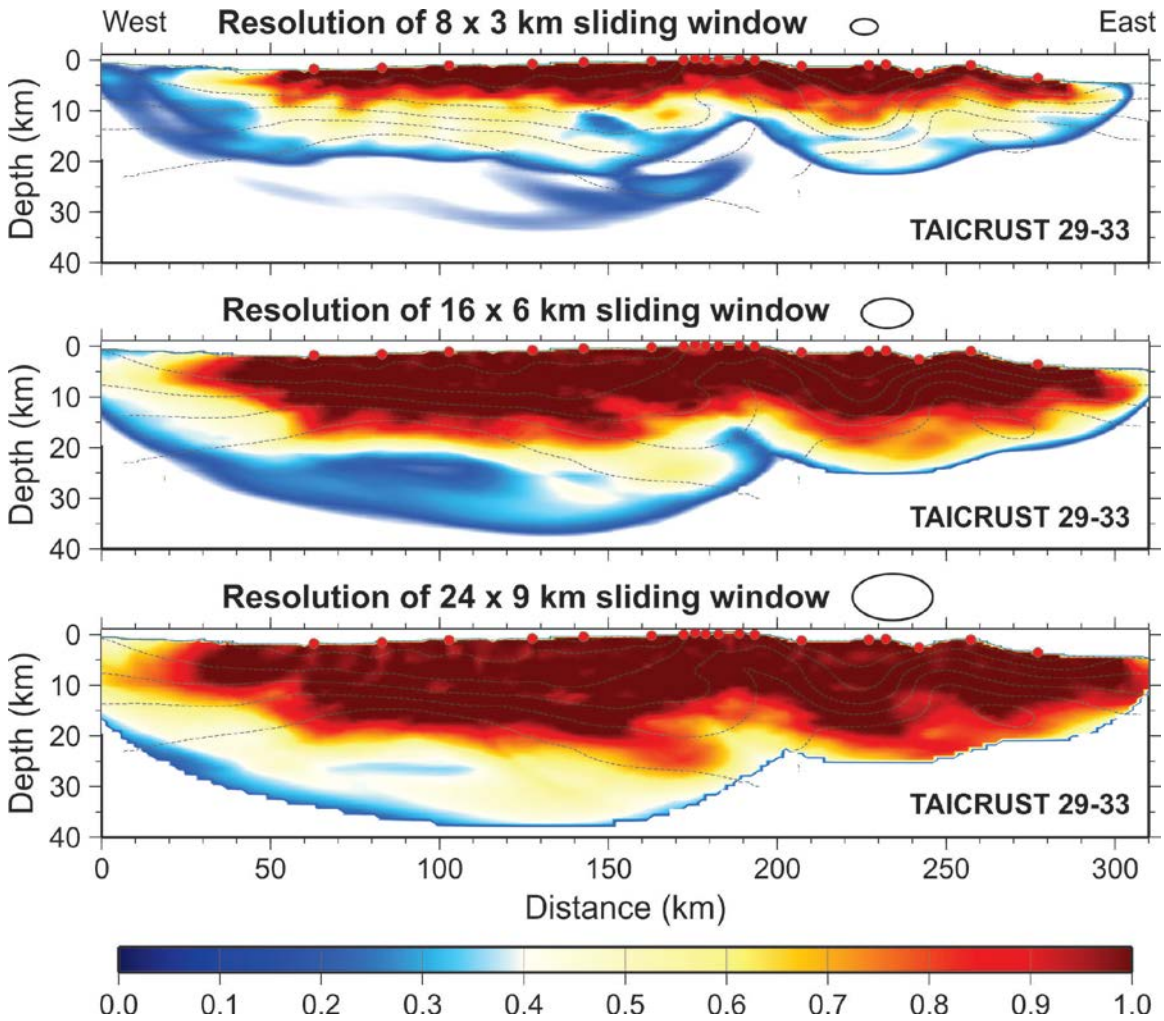

Figure DR10. Resolving power of the inversion estimated from the full resolution matrix for T2933. The resolution matrix is multiplied by sliding, elliptical windows of three different sizes to estimate how well objects of these sizes are resolved in the tomographic inversion. From top to bottom we use horizontally elongated ellipses of 8x3 km, 16x6 km, and 24x9 km. Areas with resolution values of 0.5 or greater are considered to be

sufficiently imaged. Relatively small features are well-resolved in the upper 8-10 km, while 16x6 km features are resolved through most of the sampled model, and larger features are resolved to > 30 km in the critical area beneath the Hengchun Peninsula.